https://doi.org/10.1016/j.atmosenv.2021.118298
This is the Pre-Published Version.

Characteristics, sources and evolution processes of atmospheric organic aerosols at a roadside site in Hong Kong

Dawen Yao[1], Xiaopu Lyu[1], Haoxian Lu[1], Lewei Zeng[1], Tengyu Liu[2], Chak K.Chan[3], Hai Guo[1*]

[1] Air Quality Studies, Department of Civil and Environmental Engineering, The Hong Kong Polytechnic University, Hong Kong, China

[2] Department of Chemistry, University of Toronto, Canada

[3] School of Energy and Environment, City University of Hong Kong, Hong Kong, China

Correspondence to: Hai Guo (ceguohai@polyu.edu.hk)

Abstract

A sampling campaign was conducted at an urban roadside site in Hong Kong from Nov. to Dec. in 2017 using a suite of state-of-the-art instruments to monitor compositions of non-refractory sub-micron particulate matter (NR-PM_1) and gaseous pollutants. Results showed that the average NR-PM_1 concentration was 26.1 ± 0.7 μg/m^3 (average ± 95% confidence interval) and organic aerosol (OA) contributed the most to NR-PM_1 with a proportion of 57.7 ± 0.2%. The aerosol size distributions of bulk composition of NR-PM_1 presented a peak at ~600 nm with internal mixtures of the organic and inorganic components, while there were a larger proportion of primary organic particles at < 200 nm, indicating intensive emissions of primary organics at this site. Positive matrix factorization (PMF) analysis was applied to the measurement data and four OA components were identified, including a hydrocarbon-like OA (HOA) factor, a cooking organic aerosol (COA) factor and two oxygenated OA (OOA) factors of different oxidation levels: less oxidized OOA (LO-OOA) and more oxidized OOA (MO-OOA). Strikingly, the contribution of MO-OOA was the highest (30.9 ± 0.4%), suggesting high oxidation degree and/or high regional background in the roadside environment. Moreover, the proportion of COA reached 25.4 ± 0.3% at this roadside site with heavy traffic fleet, which was even higher than the percentage of HOA (p<0.01). The average ratio of $C_3H_3O^+$ / $C_3H_5O^+$ (2.01 ± 0.01) and the opposite pattern of $C_3H_3O^+$ / $C_3H_5O^+$ to O_x during daytime hours suggested that the COA was oxidized to some extent when transported to the site. The findings implied that cooking activities are a significant source of organic aerosols in Hong Kong, even at a busy road. Control measures should focus on both cooking and traffic emissions in Hong Kong.

© 2021. This manuscript version is made available under the CC-BY-NC-ND 4.0 license http://creativecommons.org/licenses/by-nc-nd/4.0/.

Keyword: Organic aerosol; Positive matrix factorization; Cooking organic aerosol; Oxygenated organic aerosol.

1 Introduction

Atmospheric particulate matters (PM) affect climate change (Racherla et al., 2006; Tai et al., 2010) and pose a threat to public health (Dockery et al., 1993, Pope and Dockery, 2006). PM also has adverse effects on air quality and our visibility (Cheung et al., 2005; Han et al., 2016). In the atmosphere, a large fraction (20-90%) of the submicron particulate mass is organic aerosol (OA), which contains primary organic aerosol (POA) from the direct emissions of various anthropogenic and natural sources, and secondary organic aerosol (SOA) formed in the atmosphere from gas-phase precursors. Apart from local sources, the characteristics and evolution of aerosol pollution are also influenced by multiple factors such as photochemistry, meteorological parameters and regional transport (Hu et al., 2017). Thus, it is crucial to investigate the OAs in the atmosphere so that appropriate control strategies can be proposed.

With the rapid development of mass spectrometry techniques, the High Resolution - Time of Flight - Aerosol Mass Spectrometer (HR-Tof-AMS) is currently one of the most popular technologies used to identify the size-resolved abundance and composition of both organic and inorganic components of non-refractory submicron particulate matter (NR-PM_1) in the atmosphere (Jayne et al., 2000; Canagaratna et al., 2007). The HR-Tof-AMS can also provide the information of aerosols with a temporal resolution of a few minutes, which enables us to understand the quick changes and formation of aerosols (Ng et al., 2010; Hu et al., 2016). In addition, by combining the OA mass spectra gained from AMS high-resolution data with source receptor models, e.g. positive matrix factorization (PMF) model, the sources of OAs can be identified as POAs (e.g. hydrocarbon-like OA (HOA), cooking OA (COA)) and oxygenated OAs (OOAs) at each specific sampling site (Jimenez et al., 2009; Zhang et al., 2019). While HOA, COA and OOAs made substantial contributions to OAs, the proportion varied at the same site as the POAs emissions were different and the OOAs could be formed locally or transported regionally. Moreover, extensive studies have demonstrated that emissions from vehicle exhaust (Chirico et al., 2010; Nordin et al., 2013; Gordon et al., 2014a, 2014b) and cooking activities (Klein et al., 2016; Liu et al., 2017a; Liu et al., 2018) can form SOA during photochemical aging. But these studies are mostly based on chamber experiments which cannot fully represent the real environment in the atmosphere. Hence, it is still of great significance to quantify the contributions of primary emissions and secondary formation to OAs, and to further understand the formation mechanisms and the aging process of OAs in the atmosphere (Ulbrich et al., 2009; Hu et al., 2017).

Hong Kong (HK), as a highly urbanized city in East Asia, has been influenced by PM pollution in the past decades (So et al., 2007; Cheung et al., 2015). Due to large number of on-road motor vehicles and poor quality of fuel, roadside PM pollution was ever severe (Guo et al., 2009; Huang et al., 2014). However, the PM levels at roadside have been significantly reduced in recent years after the implementation of a series of control measures by the local government (HKEPD, 2017). Instead, other anthropogenic emissions, i.e. cooking activities and solvent use still cause PM pollution in HK (Lee et al., 2015; Lyu et al., 2017a). Moreover, air pollution in the adjacent Pearl River Delta (PRD) region aggravates the PM pollution in HK, particularly in autumn and winter when prevailing winds bring in polluted air masses (Louie et al., 2005; Lyu et al., 2017b). What is more, these locally-emitted and regionally-transported air pollutants can be further oxidized into SOA during dispersion and transport, resulting in elevated PM values (Hu et al., 2010). Thus, mitigating aerosol pollution in HK remains a great challenge.

A handful of OA studies using HR-Tof-AMS technique were carried out in HK (Li et al., 2013; Lee et al., 2015; Liu et al., 2017b), which help us understand the sources in different seasons and areas in HK. For instance, SOA dominated (~80 %) the organic portion of NR-PM_1 in suburban area, while POA accounted for two thirds in urban roadside area (Li et al., 2013; Lee et al., 2015). To investigate the aging processes of OAs in the atmosphere, Qin et al., (2016) summarized the episode events at a suburban site and examined the photochemical evolution of aerosols during the events. They found that the less oxidized semi-volatile oxygenated OA (SV-OOA) was clearly transformed to higher oxidized low-volatility oxygenated OA (LV-OOA) at the later stage of photochemical aging. Liu et al. (2019) investigated in-situ SOA formation from urban roadside air in HK in winter using an oxidation flow reactor (OFR) and highlighted the importance of potential SOA formation from vehicle emissions. Although a study reported that the contribution of cooking to OA and POA exceeded that of vehicle emissions at a roadside site in HK (Lee et al., 2015), the SOA formation from massive cooking emissions is still elusive and needs in-depth investigation. Therefore, it is essential to use the real-time size-resolved chemical composition data to understand the dynamic and chemical processes of aerosol evolution in the atmosphere, especially for the aerosols from cooking emissions in urban Hong Kong.

In this study, a HR-Tof-AMS together with other online instruments for real-time measurements of particulate pollutants was deployed from 2 November to 13 December 2017 at an urban roadside site in HK. The abundance, variations and size distributions of chemical components in PM_1 were firstly investigated. The characteristics and sources of OAs were then explored. Finally, the evolution processes of OA at the roadside site were elaborated. Specifically, the characteristics and evolution processes of OA, particularly COA, during high PM episode events were investigated. The findings are helpful for us to better understand the PM pollution in the roadside environment, and to provide scientific support for the remediation of organic aerosols in the atmosphere.

2 Methods and experiments

2.1 Sampling site

The sampling campaign took place between 2 November and 13 December 2017 at a location in the campus of Hong Kong Polytechnic University (PolyU) (Fig. 1). The site (22.30° N, 114.18° E) was immediately next to the eight-lane entry and exit of the Cross Harbor Tunnel, the busiest traffic junction with an average daily traffic volume of about 114,000 vehicles in 2017 (HKATC, 2017). Hence, this site is an ideal location to study the impacts of vehicular emissions on OAs. Within 1 km radius, the Tsim Sha Tsui commercial centre is located west of the sampling site, where many shops and restaurants are situated, while to the south is the Victoria Harbor. In the northeast and east of the site are residential areas with densely distributed buildings and numerous restaurants. As a metropolis, Hong Kong possess many densely populated commercial and residential areas. There are many vehicles driving on the narrow and busy canyon streets, and a lot of restaurants on both sides of the streets. Hence, the air in urban Hong Kong is full of vehicular exhaust and cooking smells. In view of the location of the sampling site and the surrounding environment, it represents a typical roadside environment in Hong Kong. Namely, vehicles and cooking activities are the main emissions in the area around the site, and there are almost no biogenic emissions nearby. The sampling inlet (~2 m long, 3.2 cm i.d.) equipped with a $PM_{2.5}$ cyclone, approximately 3.5 m above the ground, was installed on the rooftop of a container, and the air was drawn into the HR-Tof-AMS and another online instrument at a total flow rate of 16.7

L/min. Before entering the AMS, the sampled air passed through a 0.6m long diffusion dryer filled with silica gel to remove bulk gas- and particle-phase water. The residence time of less than 6s in the sampling line would reduce the loss of organic vapors (Pagonis et al., 2017). Our previous study calculated and proved the minor losses of organic vapors in the same sampling line (Liu et al., 2019).

Figure 1. Location of the sampling site and the surrounding environment

2.2 HR-Tof-AMS measurements

The NR-PM_1 compositions including organics, sulfate, nitrate, ammonium and chloride were measured using a HR-Tof-AMS. Detailed information of the instrument is described in previous AMS studies (*e.g.* Jayne et al., 2000; DeCarlo et al., 2006). In brief, an aerodynamic lens is used in AMS to sample and focus ambient particles into a narrow beam. Time zero of particle flight is defined by a rotating mechanical chopper, and the end of particle flight is defined as the time of mass spectrometric detection. Particles are transmitted to be vaporized by impaction on a resistively heated surface (~600 °C) with non-refractory species detected and measured at this vaporizer temperature and ionized by electron ionization (70 eV) (Canagaratna et al., 2007).

In this study, the HR-Tof-AMS used a Tofwerk high-resolution time-of-flight mass spectrometer (H-TOF Platform, Thun, Switzerland). The instrument was operated between two ions optical modes alternatively every 5 min, *i.e.* V-mode and W-mode. The V-mode is more sensitive while the W-mode has higher mass resolution. In V mode, 15 cycles of 10s in the mass spectrum (MS) mode (5s open and 5s closed) plus 10s in particle time-of-flight (PToF) mode yielded the size distributions of all the NR-PM_1 components in unit of mass-weighted aerodynamic diameter. In W mode, 30 cycles of 5s open and 5s closed data in MS mode were acquired before saving. The high mass resolution (~5000–6000) of the W-mode allowed us to determine the ion-specific mass spectra and thus the elemental compositions of OA (DeCarlo et al., 2006; Aiken et al., 2008; Sun et al., 2011).

The collected NR-PM_1 mass concentrations and size distribution data were treated in accordance with the general principles laid out in previous studies (Jimenez et al., 2003; DeCarlo et al., 2006), employing the standard Tof-AMS Analysis Toolkit 1.59D and Tof-AMS HR Analysis 1.19D based on WaveMetrics Igor Pro 6.37 version available from the Tof-AMS Resource Web page (http://cires.colorado.edu/jimenez-group/ToFAMSResources/ToFSoftware/index.html) and using the default relative ionization efficiency (RIE) values of 1.2 for sulfate, 1.1 for nitrate, 1.3 for chloride, and 1.4 for organics (Canagaratna et al., 2007). The RIE for ammonium was chosen as 4.3 based on the mean of RIE values obtained from the regular weekly ionization efficiency (IE) calibrations during the sampling period. By comparing with the particle mass concentrations estimated from the continuous measurement data of a scanning mobility particle sizer (SMPS, model 5.400, GRIMM, Germany) and a black carbon analyzer (BC, model AE16, Magee, USA), a collection efficiency (CE) factor of 0.7 was determined and applied to AMS-derived NR-PM_1 mass concentration (Fig. S1). Particle-free filtered ambient air was sampled using an inline HEPA-filter for about 60 min. every two days to obtain background mass spectra and the instrument minimum detection limit (MDL). The MDLs were also calculated using the background data, which were determined to be 0.201, 0.020, 0.016, 0.012, and 0.010 μg/m^3 for organic, sulfate, nitrate, ammonium and chloride, respectively. CO_2^+ signals were corrected with the time-dependent gas-phase CO_2 contributions. The contributions of organic nitrate and organic sulfate were checked and modified based on the correlation plot between the related fragments. Transmission curves for the standard lens of most AMS instruments were determined in previous study (Knote et al., 2011), which showed nearly 100% efficient transmission in the range of 100 – 550 nm and fell off at both sides. In this study, we considered the transmission efficiency as a part of the combined correction factor CE to avoid additional uncertainties from the application of non on-site calibrated lens transmission values. The elemental ratios between oxygen, carbon and hydrogen, as well as the organic mass-to-carbon ratio (OM/OC) of OA, were determined from analysis of the W-mode high-resolution mass spectra (HRMS) data, following the method recently reported by Canagaratna et al. (2015). It is noteworthy that the neglected H^+ signal from fragmentation of H_2O^+ ions may affect the oxidation state calculations. However, based on the estimation of Hildebrandt Ruiz et al. (2014), the impact was minor (< 3% variation in H:C ratio). The HR-MS data of organic aerosol were analyzed using the PMF2 algorithm in robust mode (Paatero and Tapper, 1994), with the PMF Evaluation Toolkit (PET ver 2.05) (Ulbrich et al., 2009). A minimum error value was applied to the error matrix and each ion was assessed and treated according to its signal-to-noise ratio (SNR). Ions with an average SNR of less than 0.2 were removed, and those with a SNR between 0.2 and 2 were down-weighted by increasing their errors by a factor of 2. Furthermore, ions related to m/z 44 (i.e., CO_2^+, CO^+, H_2O^+, HO^+, and O^+) were also down-weighted 2-3 times to avoid overestimating the importance of CO_2^+. Isotopes were removed from the matrices because their signals were scaled to their parent ions rather than being measured directly. After these treatments, the resulting matrix consisted of 286 ions between m/z's 12 and 120, and the number was close to previous studies (Sun et al., 2011; Kim et al., 2017).

2.3 Trace gases and meteorological measurements

Trace gases including CO, O_3, NO and NO_2 were continuously monitored during the sampling period. CO was measured with a gas filter correlation CO analyser (API model 300 EU). NO–NO_2–NO_x was measured by chemiluminescence technique (API model 200E) and an UV photometric analyzer (API model T400) was used to monitor O_3 mixing ratio. The detection limits for CO, NO, NO_2 and O_3 were 40, 0.5, 0.5 and 2.0 ppbv, respectively. All the instruments were regularly calibrated and tested with quality control and assurance (QC/QA) procedures identical to those in the US air quality monitoring program (Wang et al., 2017).

Meteorological parameters including temperature, relative humidity (RH), wind speed, wind direction, atmospheric pressure and solar radiation were measured using a weather station (Vantage Pro2TM, Davis Instruments Corp., Hayward, CA) on the rooftop of the container. The time-resolution of the measurement was 1 min., which were integrated into hourly data. The variations of hourly meteorological parameters are shown in Fig. S2. The average ambient temperature, RH, wind speed, atmospheric pressure and daily maximum solar radiation were 22.6 ± 0.2 °C, 70.2 ± 0.8%, 0.5 ± 0.02 m/s, 1017 ± 0.2 bar and 442.6 ± 65.3 W/m^2, respectively. The overall weather conditions during the sampling period were relatively stable, with only two short showers recorded. The dominant wind was a low-speed northeasterly wind, which brought in air pollutants from nearby areas.

3 Results and discussion

3.1 General characteristics

3.1.1 Temporal variations of air pollutants

The day-to-day variations and average mass concentrations of the composition of NR-PM_1 are shown in Fig. 2 ((a)-(b)). The hourly NR-PM_1 concentration ranged from 5.6 to 82.6 μg/m^3 with an average of 26.1 ± 0.7 μg/m^3 (average ± 95 confidence interval), higher than the values at other suburban and roadside sites in HK in winter, spring and/or summer (Lee et al., 2015; Li et al., 2015; Liu et al., 2019), but analogous to the levels found in autumn and early winter in HK (Sun et al., 2016), implying that this study site was more strongly affected by anthropogenic emission sources and/or weather conditions. For example, compared to the values in Liu et al. (2019) at this same sampling site, the concentrations of NR-PM_1 were indeed higher in this study. Based on the traffic volume counted (HKATC, 2017), the vehicular emissions did not have seasonal differences at this roadside site. A main reason for this difference was the weather conditions. The sampling period in Liu et al. (2019) was mainly in winter while our study period was in late autumn and early winter. A cold front over southern China moved across the coastal areas of Guangdong at the beginning of January, bringing gloomy and rainy weather to Hong Kong. The colder weather affected the formation of secondary pollutants, such as the oxidation from POA to SOA. Furthermore, the stronger northerly winds more readily diluted the air pollutants in the atmosphere of HK. For each bulk composition, though their temporal variations presented similar trends, their concentrations varied greatly. Organics was the most dominant component ranging from 3.4 to 55.8 μg/m^3 with an average of 15.1 ± 0.4 μg/m^3, accounting for 57.7 ± 0.2% of all the measured components, while sulfate was the second dominant species with an average of 5.8 ± 0.2 μg/m^3 (23.1 ± 0.2%). The concentrations of nitrate and ammonium were similar, with an average of 2.8 ± 0.2 μg/m^3 and 2.3 ± 0.1 μg/m^3, respectively.

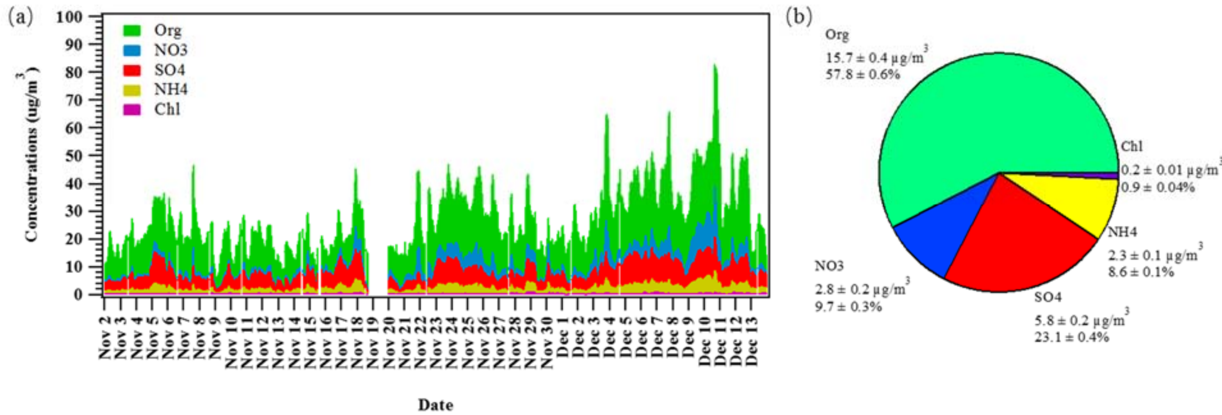

Figure 2. Day-to-day variations (a) and average composition (b) of NR-PM_1 components

The diurnal variations of NR-PM_1 and the compositions are shown in Fig. 3. The diurnal patterns of NR-PM_1 and total organics were similar (Fig. 3(a) – (b)), with the highest peak at 19:00 and two small peaks at 9:00 and 14:00, implying possible contributions of local traffic and/or cooking activities. In comparison, flat diurnal cycle of sulfate was observed (Fig. 3(d)), indicating the regional characteristics of sulfate aerosol (Sun et al., 2015). The diurnal patterns of nitrate, ammonium and chloride (Fig. 3(c), (e) – (f)) showed a trough at noon and in early afternoon, and a peak in the evening (19:00 – 20:00), consistent with the previously-observed daytime evaporation of semi-volatile species (Li et al., 2015). In addition, higher boundary layer height at noon and in the afternoon and lower ambient temperature at night also facilitated the dispersion of air pollutants and the gas–particle partitioning, respectively (Hu et al., 2017).

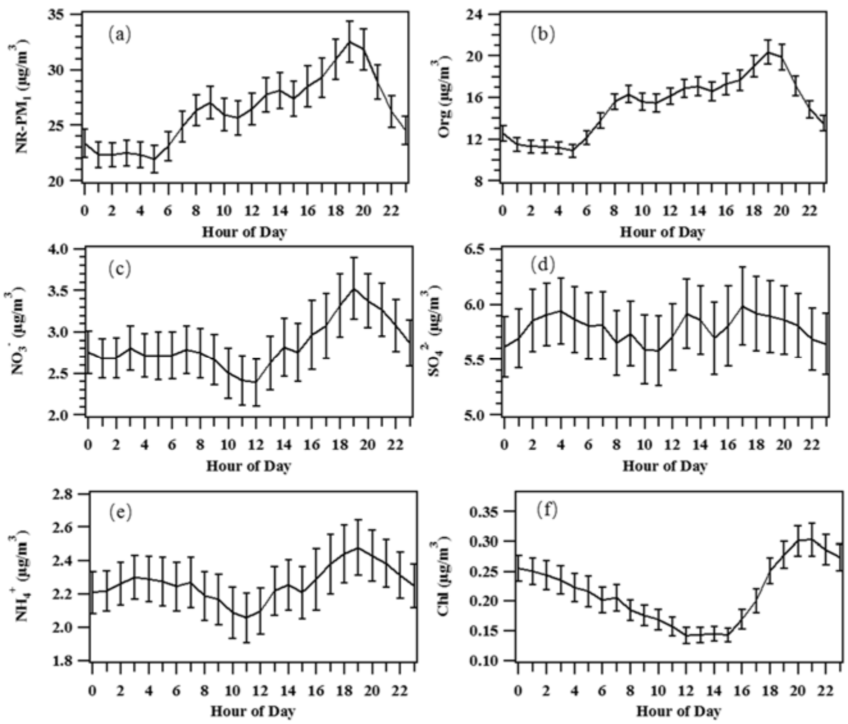

Figure 3. Diurnal variations of NR-PM$_1$ and the components

To further investigate the pollution characteristics at this site, Fig. S3 presents the diurnal variations of trace gases. Both NO and NO_2 showed a peak at 9:00, in accordance with the patterns of NR-PM$_1$ and total organics, revealing intensive vehicle emissions at this site. Noteworthily, the NO level in the evening rush hours was much lower than that in the morning, mainly due to the distinct traffic flow characteristics of vehicles in the cross-harbor tunnel (HKATC, 2017). The low evening NO level was opposite to the patterns of NR-PM$_1$ and total organics. Thus, the enhancements of NR-PM$_1$ and total organics in the evening were unlikely related to vehicular emissions but other sources such as cooking activities, which will be further discussed in Section 3.2.2. Unsurprisingly, at this typical roadside site, the O_3 levels were low with an obvious trough in the morning traffic hours due to the titration effect of NO on O_3 values. The increase in NO_2 levels from 12:00 to 16:00 also partially implied the conversion from NO titration. The CO levels were less variable except for the trough at 13:00, which was mainly due to the elevation of the boundary layer height and fewer vehicular emissions.

3.1.2 Size distributions of NR-PM$_1$ components

The size distributions of bulk compositions of NR-PM1 are shown in Fig. 4(a). All the measured non-refractory components peaked at ~600 nm in vacuum aerodynamic diameter (D_{va}), which suggested that these particles were most likely internal mixtures of the organic and inorganic components (Lee et al., 2015). Furthermore, the total organics exhibited a clear shoulder at 100–200 nm which might be caused by fresh organic aerosols of primary origin. Fig. 4(b) presents the size distributions of specific organic ions, i.e. all ions at m/z 43 (mostly $C_3H_7^+$), m/z 44 (mostly CO_2^+), m/z 55 (mostly $C_4H_7^+$ and $C_3H_3O^+$) and m/z 57 (mostly $C_4H_9^+$ and $C_3H_5O^+$). These specific ions were selected as they had remarkable peaks in the spectra. It was found that hydrocarbon-like organics (m/z 43, 55, 57) had higher concentrations at sizes of 100–200 nm than m/z 44 (p<0.01). The small peaks of these typical ions were also found in previous studies, indicating a large contribution of hydrocarbon-like organics from primary emissions such as traffic to the total organics (Canagaratna et al., 2010; Sun et al., 2011).

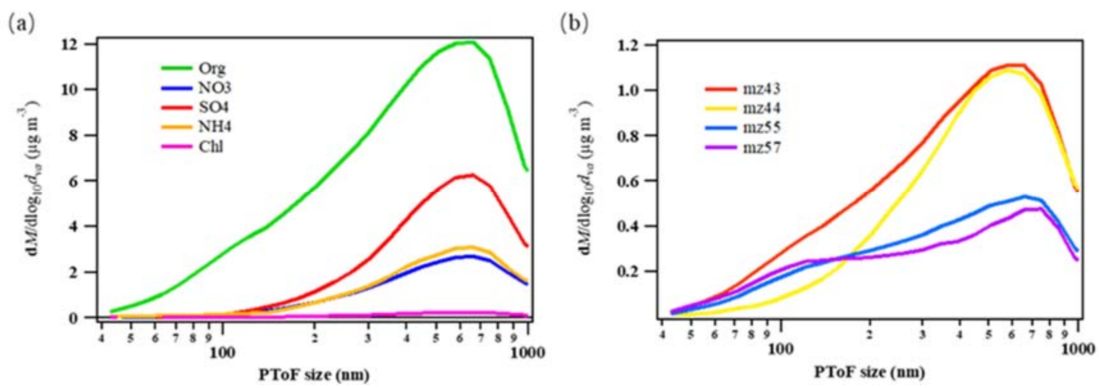

Figure 4. Size distributions of bulk compositions (a) and specific m/z ions (b)

3.1.3 Elemental ratios of OAs

There are several ways to evaluate the degree of OA oxygenation using AMS data (Aiken et al., 2008; Heald et al., 2010; Kroll et al., 2011). The hydrogen-to-carbon molar ratios (H:C) and oxygen-to-carbon molar ratios (O:C) are often used to estimate the average carbon oxidation state (OS_C) and to evaluate the degree of oxygenation of organics. Based on the measurements of H:C and O:C ratios, the OS_C value can be simply calculated as 2 × O:C – H:C, which more accurately captures the degree of oxidation of organics than the O:C ratio (Kroll et al., 2011). Fig. 5 shows the diurnal patterns of elemental ratios in this study. The average organic mass to organic carbon ratios (OM:OC), O:C and H:C ratios were 1.77 ± 0.01, 0.47 ± 0.01 and 1.69 ± 0.01, respectively. These values are comparable with the H:C (1.4 - 1.9) and O:C ratios (0.2 - 0.8) previously measured at urban roadside sites in HK, perhaps due to the similar emission sources at these sites (Lee et al., 2015; Liu et al., 2019). The H:C ratio was low in the evening, had a morning peak at 9:00-10:00 with a value of 1.79 ± 0.02, and then decreased with time until 21:00 when a small evening peak appeared, suggesting more intensive primary emissions (e.g. traffic and cooking) in these peak hours and photochemical oxidation of organics in the afternoon and/at dusk, which were proved by the opposite diurnal trend of the O:C ratio; namely troughs at 9:00-10:00 and 21:00 and increase in the afternoon and at dusk. The dramatic decrease of POA emissions at night led to a higher proportion of secondary OA, so the O:C ratio from 1:00 to 6:00 was the highest. Meanwhile, OS_C showed an evening peak and an afternoon peak, with an average of -0.76 ± 0.02 during the whole sampling period.

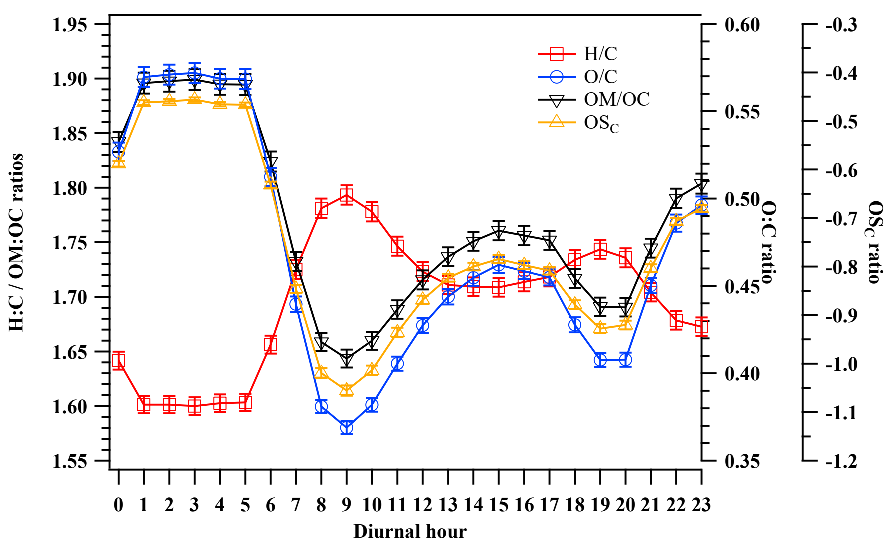

Figure 5. Diurnal patterns of OM:OC, H:C, O:C and OS_C ratios.

3.2 Source apportionment of OAs

3.2.1 Source identification

In order to obtain physically meaningful results, several criteria were used to evaluate and select appropriate number of factors from model simulation in this study (Ulbrich et al., 2009; Zhang et al., 2011; Kim et al., 2017). Fig. S4(a) shows the Q/Q_{exp} values for factors 1-6. The Q/Q_{exp} values decreased with the increase of number of factors, and the possible optimal solution should be 6 or more factors. However, when the source profiles of 5 factors are compared (Fig. S4 (b)), it was found that the two OOA factors had similar spectra and close elemental ratios. In addition, after consideration of the elucidation of the mass spectra of OAs, the ability of 5 factors or more to explain the data was not improved compared to 4 factors. Hence, the solution of 4 factors was the most optimal solution. The rotational ambiguity of the optimal solution was examined by the FPEAK value, which ranged from -2 to 2. The uncertainty of each factor was estimated by 50 bootstrapping runs, and the average factor with 1σ variation for each point is shown in Fig. S4 (c). It is noteworthy that Liu et al. (2019) identified 5 factors at the same site for the campaign, which started 11 days after the campaign in this study. The reason for this difference was that the OA levels and atmospheric oxidative capacity during this sampling period were generally higher. As such, the less oxidized OA factor with the lowest contribution in Liu et al. (2019) was not identified in this study. The similar diel cycles of the four factors in our study to the rest factors in Liu et al. (2019) showed the consistency and reliability of the results, which will be further discussed in section 3.2.2.

In this study, four OA factors were determined, including two POA factors (HOA and COA) and two SOA factors (less oxidized oxygenated OA (LO-OOA) and more oxidized OOA (MO-OOA)). The mass spectra of the four identified factors are shown in Fig. 6. Table 1 gives the H:C, O:C and OM:OC ratios of the MO-OOA, LO-OOA, COA and HOA factors. Alkyl fragments ($C_nH_{2n+1}^+$ and $C_nH_{2n-1}^+$) made a substantial contribution to the HOA factor. The major peaks of HOA mass spectrum were m/z 41, 43, 55 and 57, which were mostly composed of $C_3H_5^+$, $C_3H_7^+$, $C_4H_7^+$ and $C_4H_9^+$ ions, respectively. These major peaks and the overall abundant alkyl fragments are the typical features of the HOA spectra. This fragmentation pattern was similar to that reported in other studies and was mainly due to the primary aerosols emitted from fossil fuel combustion (Zhang et al., 2005; Lanz et al., 2008; Ng et al., 2011; Sun et al., 2011). Because of the dominance of chemically-reduced hydrocarbon species, HOA factor had the highest H:C ratio (average: 2.10), and conversely the lowest O:C (0.03) and OM:OC (1.22) ratios. The oxidation degree of the HOA in this study was comparable to the updated values of HOA (O:C ratio: 0.05–0.25) from other studies (Canagaratna et al., 2015). The relatively low O:C ratio was mainly due to the intensive primary emissions from vehicle exhausts at this roadside site.

To a lesser extent, the mass spectrum of COA factor in this study also contained many alkyl fragments. However, this factor had significantly larger amounts of oxygen-containing ions than HOA. While COA shares similar spectra to HOA, it is identified by a high contribution of $C_3H_3O^+$ at m/z 55, and a much lower contribution of ions at m/z 57 than HOA (Mohr et al., 2009; Mohr et al., 2012). Previous studies found that $C_3H_3O^+$ and $C_3H_5O^+$ are in COA as they are the major fragments of aliphatic acids (e.g., linoleic acid and palmitic acid) in cooking oils or animal fat (Sun et al., 2011). It was also reported that $C_5H_8O^+$ (m/z 84) and $C_6H_{10}O^+$ (m/z 98) are the typical tracers in COA (Lee et al., 2015; Kim et al., 2017). Fig. S5 (a)-(h) shows the scatter plots of COA and HOA with the cooking tracers ($C_3H_3O^+$, $C_3H_5O^+$, $C_5H_8O^+$and $C_6H_{10}O^+$). It was obvious that the COA concentration had much better correlations than HOA with these four cooking tracers, confirming that the second source was COA. Despite primary origins for both factors, COA was more oxidized than HOA because it contained some oxidizing components as discussed above. Therefore, the O:C (0.22) and OM:OC (1.45) ratios of COA were higher than those of HOA while the H:C ratio was lower (1.88). Besides, Xu et al. (2018) revealed that COA may include contribution of other OA such as sesquiterpene SOA. In this study, there was almost no biogenic emissions and other sources except vehicular and cooking emissions around the sampling site, which would exclude the interference from biogenic emissions and other sources. In fact, relatively weaker correlation between COA source and the tracer of biogenic emissions, i.e. $C_5H_6O^+$ at m/z 82 was identified (Fig. S6), confirming that COA was less interfered by other OAs at this site.

In this study, the two identified OOA factors had less alkyl fragments and more oxygenated species than the HOA and COA. The mass spectra of the two OOAs were characterized by a dominant peak at m/z 44 (CO_2^+), similar to the OOA profiles determined in other studies (Lanz et al., 2007; Ulbrich et al., 2009; Sun et al., 2010, 2011). To distinguish these two OOA factors, it was found that the third factor had a lower fraction of m/z 44 (f44) and less oxidation degree (O:C = 0.78, H:C = 1.53) than the fourth factor (O:C = 0.97, H:C = 1.40). As such, Factor 3 was characterized as LO-OOA while Factor 4 was defined as MO-OOA.

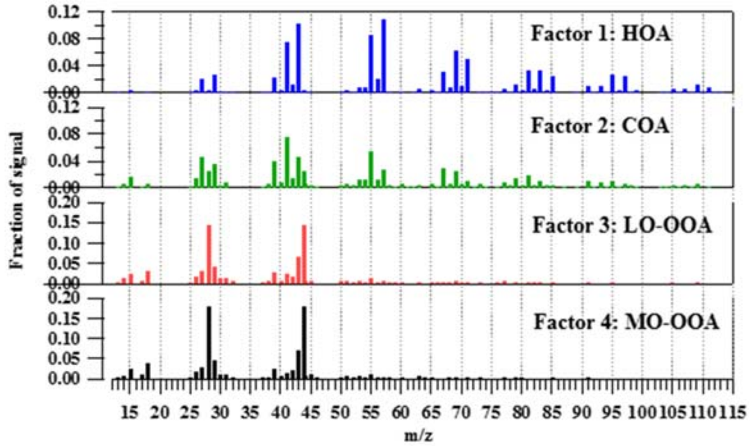

Figure 6. Sources profiles of the four factors

Table 1 Elemental ratios of the four factors

	HOA	COA	LO-OOA	MO-OOA
H:C	2.10	1.88	1.53	1.40
O:C	0.03	0.22	0.78	0.97
OM:OC	1.22	1.45	2.18	2.41

3.2.2 Source contributions

Fig. 7(a) presents the contribution of each identified source to OAs in both absolute concentration and percentage. Surprisingly, although this roadside site was proximity to intensive vehicular sources, the contribution of MO-OOA was the highest, followed by COA and LO-OOA, while the contribution of HOA was the lowest. The SOA sources (LO-OOA+MO-OOA) contributed more than the POA sources (COA+HOA), which is consistent with the result of Liu et al. (2019) who collected data at the same site, implying possibly prompt oxidation of OAs and/or high regional background at the roadside site. Moreover, the contribution of LO-OOA was lower than MO-OOA (p<0.01), suggesting high oxidation degree and/or high regional background in the roadside environment. More striking feature was that the contribution of COA was even higher than that of

HOA (p<0.01) at this site with very high-density passing vehicles and very few restaurants nearby. This phenomenon implied that the control of vehicular emissions might be efficient while the COA-containing air was full of the urban environment including the roadside environment in HK. Our previous studies found that volatile organic compounds (VOCs) emitted from diesel-fuelled and LPG-fuelled vehicles have dropped during these years due to the control measures in HK (Lyu et al., 2016, 2017a; Yao et al., 2019), whereas VOCs from gasoline-fuelled vehicles have shown an increasing trend. However, these studies did not measure OAs. Instead, OAs were measured in 2013 at an urban roadside site, i.e. Mong Kok (MK). Similar to the study site, the MK site is also a typical urban roadside site with heavy traffic and minimal biogenic emissions. In comparison, the HOA concentration at MK (2.7 μg/m^3, Table 2) was comparable to that in this study (2.8 ± 1.9 μg/m^3, Table 2) in the same season (autumn and early winter). The comparable HOA values at the roadside sites in different years seemed contradictory to the results of the previous studies, which claimed the efficiency of control measures for vehicular emissions. However, if we looked deeper into the HOA values and considered the traffic volume at MK and at the Cross-Harbor tunnel, we found that the HOA level associated with each vehicle indeed decreased twice from 2013 to 2019, because the average daily traffic of the main road (Nathan Road) immediately next to the MK site was ~50,000, much less than the traffic volume of ~114,000 at the Cross-Harbor tunnel (HKATC, 2017). In addition, it was found that regardless of the season and sampling location, the level of COA was always higher than that of HOA, which further indicated that cooking emissions were more dominant than vehicle emissions even in heavy traffic locations (Table 2).

Regarding the diurnal variations of the contributions of the four sources, the HOA source showed a high peak at 9:00 and a small peak at 17:00-18:00 (Fig. 7(b)), analogous to the pattern of NO due to road traffic (Fig. S3). Similarly, two peaks were found for COA source with a small peak at 12:00-13:00 and a big peak at 20:00 (8.2 ± 0.8 μg/m^3). The contrary pattern of NO (Fig. S3) and similar variations of NR-PM$_1$ and total organics (Fig. 3) to the COA source in the evening, which is in line with the dinner time in HK (Lee et al., 2015; Vu et al., 2018), supported the identification of the COA source. To further clarify the cooking emissions at this site, the diurnal pattern of oleic acid, a typical tracer of cooking activities (Schauer et al., 2002; Zhao et al., 2007), measured at PolyU (~300 m away from the sampling site) is shown in Fig. S7. It was clear that the peak value appeared at 20:00, consistent with the diurnal variation of COA source, confirming the intensive cooking emissions during the dinner time in urban HK. Furthermore, the LO-OOA source presented a bimodal distribution with a peak at 9:00 and another broad peak at 17:00-18:00, which was coincidently opposite to the O_3 pattern, indicating immediate morning formation of LO-OOA from HOA of vehicular exhausts and progressive oxidation in the afternoon (Sun et al., 2016). However, the MO-OOA source was relatively constant throughout the day, inconsistent with the patterns of all the trace gases in Fig. S3, confirming high regional background value of this source.

The variations of the percentages of individual sources in the sum of PMF-resolved OAs are shown in Fig. 7(c). It was found that the percentage of COA increased with the increase of total PMF-resolved OAs, implying that COA was the major contributor when OA levels were high. HOA showed the same pattern as COA but its increasing rate was much lower than that of COA. In contrast, the percentage of MO-OOA decreased while LO-OOA remained stable.

To further investigate the HOA and COA sources, the diurnal trends of them on Saturday, Sunday and weekdays are given (Fig. 7(d)). A much higher HOA morning peak was found on weekdays and Saturday (p<0.01), whereas COA presented a much higher evening peak on Sunday (p<0.01), consistent with the fact that there are much fewer on-road vehicles and much more Hong Kong residents like to have dinner at restaurants on Sunday (Chan, 2010). Indeed, the contribution of COA on Sunday to the overall COA concentration reached 22.3% in this study. Moreover, the COA levels were much higher than the HOA concentrations (p<0.01). Although it is difficult to differentiate the emissions from restaurants from those from domestic cooking due to lack of survey data, we can infer that emissions from restaurants were much higher on Sunday than on other days, and most likely larger than domestic cooking emissions from the big difference in peak values of COA on Sunday (~15 μg/m^3) and on the other days (~6 μg/m^3) (Fig. 7(d)). The results suggested that cooking activities particularly in restaurants are a noticeable source of OAs in Hong Kong and much more efforts should be made to control it apart from remediation of vehicular emissions.

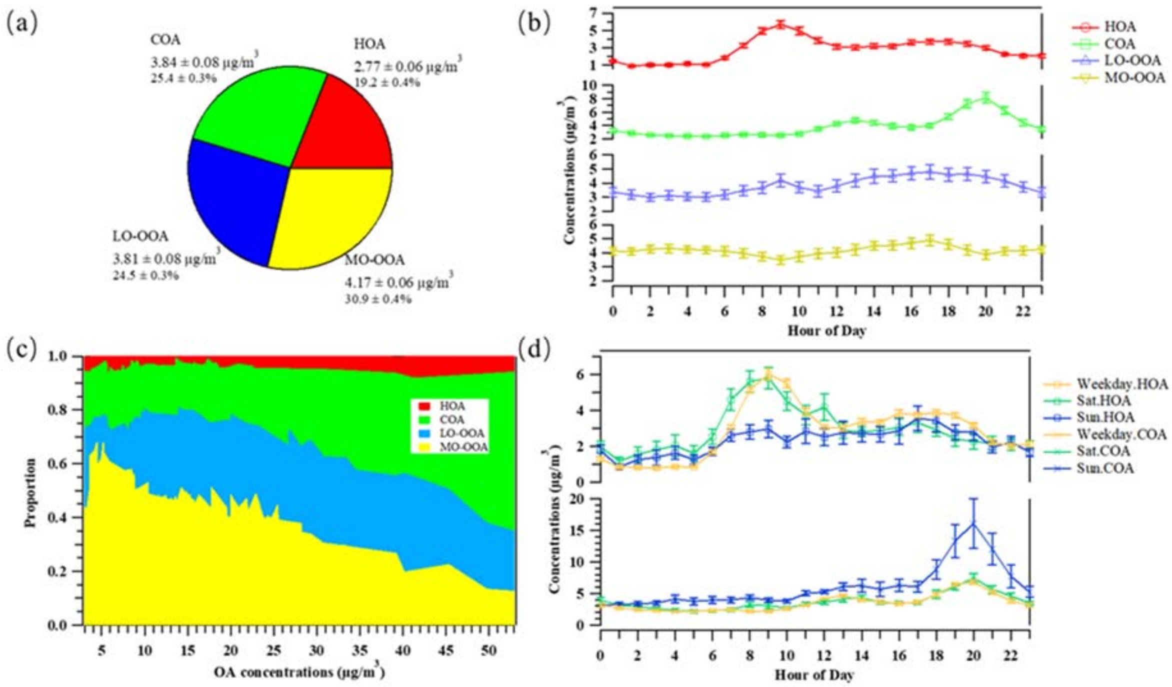

Figure 7. (a) Source contributions to OAs. (b) Diurnal patterns of the OA sources. (c) Percentage variations of individual sources in the sum of PMF-resolved OAs. The values of the x-axis represent the hourly OA concentrations measured. (d) Diurnal patterns of HOA and COA on Saturday, Sunday and weekdays.

Table 2 HOA and COA levels in urban roadside environments in HK (mean ± standard deviation)

Time	Sampling time	Site	HOA concentration (µg/m^3)	COA concentration (µg/m^3)	COA proportion
Nov. - Dec. 2017, This study	24h	PolyU	2.8 ± 1.9	3.8 ± 2.9	25.4 ± 1.0
	Mealtime	PolyU	3.0 ± 1.4	5.8 ± 4.0	33.5 ± 10.6
Mar. - May 2013 (Lee et al., 2017)	24h	MK	3.5 ± 2.4	4.4 ± 4.3	34.4
May - Jul. 2013 (Lee et al., 2017)	24h	MK	2.0 ± 1.3	3.6 ± 3.4	46.2
Mar. - Jul. 2013 (Lee et al., 2015)	24h	MK	2.8	4.0	38.6
Sep. - Dec. 2013	24h	MK	2.7	3.6	24.2
(Sun et al., 2016)	Mealtime	MK	3.2	7.8	36.9

3.3 Evolution of OA sources

Typical ions are usually chosen to study the evolution of a specific OA source. Long straight-chain fatty acids, including unsaturated (*e.g.* oleic acid and linoleic acid) and saturated (*e.g.* palmitic acid and stearic acid), are unique markers for cooking emissions as they are from oils during cooking processes (He et al., 2004; Zhao et al., 2007). Based on the source profile of COA (Mohr et al., 2012), and the strong correlations with COA factor in this study (Fig. S5), here $C_3H_3O^+$ at m/z 55 and $C_3H_5O^+$ at m/z 57 were chosen as the proxy of unsaturated fatty acids and saturated fatty acids, respectively. In addition, ion CO_2^+ at m/z 44 was regarded as the typical tracer of OOA as it had strong correlations with the OOA sources ($R > 0.9$). The diurnal patterns of $C_3H_3O^+$, $C_3H_5O^+$ and CO_2^+ are shown in Fig. 8(a). The diel cycles of $C_3H_3O^+$ and $C_3H_5O^+$ were the same as that of COA source (Fig. 8(a)), confirming their common source of cooking emissions. Different from $C_3H_3O^+$ and $C_3H_5O^+$, CO_2^+ presented a broad peak starting from 10:00 and maximizing at 17:00, suggesting the photochemical oxidation of OAs in the atmosphere.

To further look into the oxidation of OAs at this roadside site, the diurnal patterns of $C_3H_3O^+$/ $C_3H_5O^+$ ratio and total oxidant ($O_x = O_3 + NO_2$) are illustrated in Fig. 8(b). The ratio of $C_3H_3O^+$ / $C_3H_5O^+$ was used to elaborate the oxidation degree of cooking emissions in the atmosphere, because unsaturated fatty acids (*i.e.* $C_3H_3O^+$) have shorter lifetime than saturated fatty acids (*i.e.* $C_3H_5O^+$), which means that unsaturated fatty acids are photochemically destroyed more rapidly than saturated fatty acids, leading to decline of $C_3H_3O^+$ / $C_3H_5O^+$ ratio. Besides, the level of O_x was used to characterize the atmospheric oxidative capacity (Clapp and Jenkin, 2001). The diurnal variation of $C_3H_3O^+$ / $C_3H_5O^+$ ratio showed one peak at 13:00 (2.04 ± 0.01) and another at 20:00 (2.17 ± 0.01), in consistence with that of cooking emissions. Clearly, during the daytime hours, the ratio of $C_3H_3O^+$ / $C_3H_5O^+$ showed opposite trend to that of O_x, proving the evolution of cooking emissions in the atmosphere. However, the reversed pattern was not observed in the evening even though the cooking emissions reached the highest, reflecting that the nighttime chemical evolution of cooking emissions on average was insignificant. In addition, the average ratio of $C_3H_3O^+$ / $C_3H_5O^+$ during the whole sampling period was 2.01 ± 0.01, much lower than the ratio of oleic acid/stearic acid (4.8) of the cooking source (Zhao et al., 2007), implying that COA was oxidized to some extent during the transport to the site. Furthermore, the average O_x level during the sampling period was 56.0 ± 1.4 ppbv, analogous to the values (55.9 ± 3.4 ppbv) at another roadside site in HK (Yao et al., 2019). Previous studies reported that COA could be oxidized in an hour under a moderate O_3 level (Kaltsonoudis et al., 2017). The reversed daytime patterns of $C_3H_3O^+$ / $C_5H_5O^+$ and O_x in this study confirmed this hypothesis, especially in the afternoon when the photochemical reactions were generally strong. The results demonstrated that the COA emitted elsewhere was progressively oxidized, leading to enhanced OOA at this roadside site.

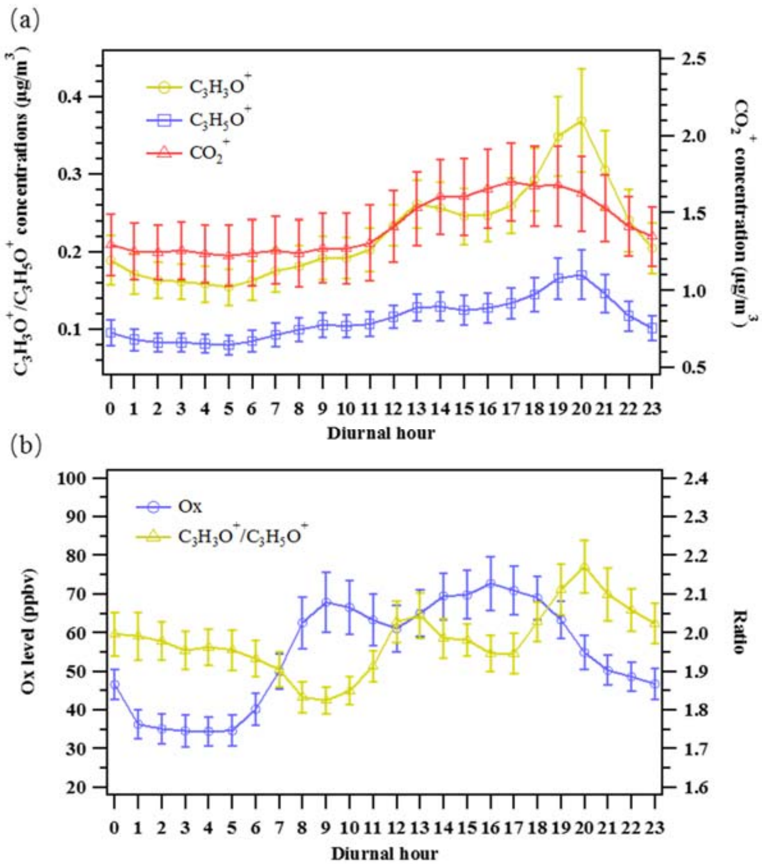

Figure 8. Diurnal variations of $C_3H_3O^+$, $C_3H_5O^+$ and CO_2^+ (a) and ratio of $C_3H_3O^+$ / $C_3H_5O^+$ and O_x (b) during the whole sampling period

4 Conclusions

In this study, an intensive sampling campaign was conducted for six weeks at a roadside site in Hong Kong. HR-Tof-AMS and trace gas analyzers (*i.e.* CO, O_3 and NO-NO_2-NO_x) were used to collect data simultaneously to investigate and understand the characteristics, sources and evolution processes of OAs in the roadside environment. Results showed that the average NR-PM_1 concentration was 26.1 ± 0.7 μg/m^3 and OA contributed the most to NR-PM_1 with the proportion of 57.7 ± 0.2%. The aerosol size distributions of all measured NR-species showed an accumulation mode peaked at around 600 nm while there were more primary organics at < 200 nm. PMF analysis identified four OA components (HOA, COA, LO-OOA and MO-OOA), and the proportion of COA was 25.4 ± 0.3%, even higher than that of HOA (19.2 ± 0.4%) at this traffic-busy site. The COA concentration reached the highest value at 20:00 with an average of 8.2 ± 0.8 μg/m^3. Especially on Sundays, the average maximum COA concentration was 16.1 ± 3.0 μg/m^3. Furthermore, with the increase of PMF-resolved total OA concentrations, the proportion of COA increased. The ratio of $C_3H_3O^+$ / $C_3H_5O^+$ was used to elaborate the oxidation degree of cooking emissions in the atmosphere, and the daytime opposite trend of the ratio of $C_3H_3O^+$ / $C_3H_5O^+$ to that of O_x confirmed the evolution of cooking emissions in the atmosphere. This study concludes that cooking activities are an important source of organic aerosols in the urban areas of Hong Kong, and efforts should be made to control emissions from cooking and traffic.

Acknowledgements

This study was supported by the Research Grants Council of the Hong Kong Special Administrative Region via Theme-Based Research Scheme (Project T24-504/17-N) and General Research Fund (PolyU 152052/16E), and the Strategic Focus Area scheme of The Research Institute for Sustainable Urban Development at The Hong Kong Polytechnic University (1-BBW9), and the Hong Kong Polytechnic University internal fund (4-BCF6).

References

Aiken, A. C., DeCarlo, P. F., Kroll, J. H., Worsnop, D. R., Huffman, J. A., Docherty, K. S., Ulbrich, I. M., Mohr, C., Kimmel, J. R., Sueper, D., Sun, Y., Zhang, Q., Trimborn, A., Northway, M., Ziemann, P. J., Canagaratna, M. R., Onasch, T. B., Alfarra, M. R., Prevot, A. S. H., Dommen, J., Duplissy, J., Metzger, A., Baltensperger, U., and Jimenez, J. L.: O/C and OM/OC ratios of primary, secondary, and ambient organic aerosols with High-Resolution Time-of-Flight Aerosol Mass Spectrometry, Environ. Sci. Technol., 42, 4478–4485, doi: 10.1021/es703009q, 2008.

Canagaratna, M. R., Jayne, J. T., Jimenez, J. L., Allan, J. D., Alfarra, M. R., Zhang, Q., Onasch, T. B., Drewnick, F., Coe, H., Middlebrook, A., Delia, A., Williams, L. R., Trimborn, A. M., Northway, M. J., DeCarlo, P. F., Kolb, C. E., Davidovits, P., and Worsnop, D. R.: Chemical and microphysical characterization of ambient aerosols with the aerodyne aerosol mass spectrometer, Mass Spectrom. Rev., 26, 185-222, doi: 10.1002/mas.20115, 2007.

Canagaratna, M. R., Onasch, T. B., Wood, E. C., Herndon, S. C., Jayne, J. T., Cross, E. S., Miake-Lye, R. C., Kolb, C. E., and Worsnop, D. R.: Evolution of vehicle exhaust particles in the atmosphere, J. Air Waste Manage. Assoc., 60, 1192–1203, doi: 10.3155/1047-3289.60.10.1192, 2010.

Canagaratna, M. R., Jimenez, J. L., Kroll, J. H., Chen, Q., Kessler, S. H., Massoli, P., Hildebrandt Ruiz, L., Fortner, E., Williams, L. R., Wilson, K. R., Surratt, J. D., Donahue, N. M., Jayne, J. T., and Worsnop, D. R.: Elemental ratio measurements of organic compounds using aerosol mass spectrometry: characterization, improved calibration, and implications, Atmos. Chem. Phys., 15, 253- 272, doi:10.5194/acp-15-253-2015, 2015.

Chan, H.: Removal and recycling of pollutants from Hong Kong restaurant wastewaters, Bioresour. Technol., 17, 6859-6867, doi: 10.1016/j.biortech.2010.03.104, 2010.

Cheung, H. C., Wang, T., Baumann, K., and Guo, H.: Influence of regional pollution outflow on the concentrations of fine particulate matter and visibility in the coastal area of southern China, Atmos. Environ., 39, 6463-6474, doi: 10.1016/j.atmosenv.2005.07.033, 2005.

Cheung K, Ling Z. H., Wang D. W., Wang Y, Guo H., Lee B., Li Y. J., and Chan C. K.: Characterization and source identification of sub-micron particles at the HKUST Supersite in Hong Kong, Sci. Total Environ., 527-528, 287-296, doi: 10.1016/j.scitotenv.2015.04.087, 2015.

Chirico, R., DeCarlo, P. F., Heringa, M. F., Tritscher, T., Richter, R., Prévôt, A. S. H., Dommen, J., Weingartner, E., Wehrle, G., Gysel, M., Laborde, M. and Baltensperger, U.: Impact of aftertreatment devices on primary emissions and secondary organic aerosol formation potential from in-use diesel vehicles: results from smog chamber experiments, Atmos. Chem. Phys., 10, 11545-11563, doi: 10.5194/acp-10-11545-2010, 2010.

Clapp, L. J., and Jenkin, M. E.: Analysis of the relationship between ambient levels of O_3, NO_2 and NO as a function of NO_x in the UK, Atmos. Environ., 35, 6391-6405, doi: org/10.1016/S1352-2310(01)00378-8, 2001.

DeCarlo, P. F., Kimmel, J. R., Trimborn, A., Northway, M. J., Jayne, J. T., Aiken, A. C., Gonin, M., Fuhrer, K., Horvath, T., Docherty, K. S., Worsnop, D. R., and Jimenez, J. L.: Field-deployable, high-resolution, time-of-flight aerosol mass spectrometer, Anal. Chem., 78, 8281-8289, doi: 10.1021/ac061249n, 2006.

DeCarlo, P. F., Dunlea, E. J., Kimmel, J. R., Aiken, A. C., Sueper, D., Crounse, J., Wennberg, P. O., Emmons, L., Shinozuka, Y., Clarke, A., Zhou, J., Tomlinson, J., Collins, D. R., Knapp, D., Weinheimer, A. J., Montzka, D. D., Campos, T., and Jimenez, J. L.: Fast airborne aerosol size and chemistry measurements above Mexico City and Central Mexico during the MILAGRO campaign, Atmos. Chem. Phys., 8, 4027–4048, doi: org/10.5194/acp-8-4027-2008, 2008.

DeCarlo, P. F., Ulbrich, I. M., Crounse, J., de Foy, B., Dunlea, E. J., Aiken, A. C., Knapp, D., Weinheimer, A. J., Campos, T., Wennberg, P. O., and Jimenez, J. L.: Investigation of the sources and processing of organic aerosol over the Central Mexican Plateau from aircraft measurements during MILAGRO, Atmos. Chem. Phys., 10, 5257–5280, doi: 10.5194/acp-10-5257-2010, 2010.

de Gouw, J. and Jimenez, J. L.: Organic aerosols in the Earth's atmosphere, Environ. Sci. Technol., 43, 7614–7618, doi: 10.1021/es9006004, 2009.

Dockery, D. W., Pope, C. A., Xu, X., Spengler, J. D., Ware, J. H., Fay, M. E., Ferris, B. G. and Speizer, F. E.: An association between air pollution and mortality in six US cities, N. Engl. J. Med., 329, 1753-1759, doi: 10.1056/NEJM199312093292401, 1993.

Gordon, T. D., Presto, A. A., Nguyen, N. T., Robertson, W. H., Na, K., Sahay, K. N., Zhang, M., Maddox, C., Rieger, P., Chattopadhyay, S., Maldonado, H., Maricq, M. M. and Robinson, A. L.: Secondary organic aerosol production from diesel vehicle exhaust: impact of aftertreatment, fuel chemistry and driving cycle, Atmos. Chem. Phys., 14, 4643-4659, doi: 10.5194/acp-14-4643-2014, 2014a.

Gordon, T. D., Presto, A. A., May, A. A., Nguyen, N. T., Lipsky, E. M., Donahue, N. M., Gutierrez, A., Zhang, M., Maddox, C., Rieger, P., Chattopadhyay, S., Maldonado, H., Maricq, M. M. and Robinson, A. L.: Secondary organic aerosol formation exceeds primary particulate matter emissions for light-duty gasoline vehicles, Atmos. Chem. Phys., 14, 4661-4678, doi: 10.5194/acp-14-4661-2014, 2014b.

Guo, H., Ding, A. J., So, K. L., Ayoko, G., Li, Y. S., and Hung, W. T.: Receptor modeling of source apportionment of Hong Kong aerosols and the implication of urban and regional contribution, Atmos. Environ., 43, 1159-1169, doi: 10.1016/j.atmosenv.2008.04.046, 2009.

Han, L., Zhou, W., and Li, W.: Fine particulate ($PM_{2.5}$) dynamics during rapid urbanization in Beijing, 1973–2013, Sci. Rep., 6, 23604, doi: 10.1038/srep23604, 2016.

He, L. Y., Hu, M., Huang, X. F., Yu, B. D., Zhang, Y. H., and Liu, D. Q.: Measurement of emissions of fine particulate organic matter from Chinese cooking, Atmos. Environ., 38, 6557-6564, doi: 10.1016/j.atmosenv.2004.08.034, 2004.

Heald, C. L., Kroll, J. H., Jimenez, J. L., Docherty, K. S., DeCarlo, P. F., Aiken, A. C., Chen, Q., Martin, S. T., Farmer, D. K., and Artaxo, P.: A simplified description of the evolution of organic aerosol composition in the atmosphere, Geophys. Res. Lett., 37, L08803, doi:10.1029/2010gl042737, 2010.

Hildebrandt Ruiz, L., Paciga, A. L., Cerully, K., Nenes, A., Donahue, N. M., and Pandis, S. N.: Aging of secondary organic aerosol from small aromatic VOCs: changes in chemical composition, mass yield, volatility and hygroscopicity, Atmos. Chem. Phys. Discuss., 14, 31441–31481, doi:10.5194/acpd-14-31441-2014, 2014.

Hong Kong Annual Traffic Census 2017 Edition (HKATC). Accessible at: https://www.td.gov.hk/filemanager/en/content_4915/annual%20traffic%20census%202017.pdf, 2017.

Hong Kong Environmental Protection Department (HKEPD), Air Quality in Hong Kong 2017, Accessible at http://www.aqhi.gov.hk/api_history/english/report/files/AQR2017e_final.pdf, 2017.

Hu, D., Bian, Q., Lau, A. K., and Yu, J. Z.: Source apportioning of primary and secondary organic carbon in summer PM2.5 in Hong Kong using positive matrix factorization of secondary and primary organic tracer data, J. Geophys. Res., 115, D16204, doi: 10.1029/2009JD012498, 2010.

Hu, W., Hu, M., Hu, W., Jimenez, J. L., Yuan, B., Chen, W., Wang, M., Wu, Y., Chen, C., Wang, Z., Peng, J., Zeng, L., and Shao, M.: Chemical composition, sources and aging process of sub-micron aerosols in Beijing: contrast between summer and winter, J. Geophys. Res., 121, 1955–1977, doi: 10.1002/2015JD024020, 2016.

Hu, W., Hu, M., Hu, W. W., Zheng, J., Chen, C., Wu, Y., and Guo, S.: Seasonal variations in high time-resolved chemical compositions, sources, and evolution of atmospheric submicron aerosols in the megacity Beijing, Atmos. Chem. Phys., 17, 9979-10000, doi: 10.5194/acp-17-9979-2017, 2017.

Huang, X. H., Bian, Q. J., Louie, P. K., and Yu, J. Z.: Contributions of vehicular carbonaceous aerosols to PM2.5 in a roadside environment in Hong Kong, Atmos. Chem. Phys., 14, 9279-9293, doi: 10.5194/acp-14-9279-2014, 2014.

Jayne, J. T., Leard, D. C., Zhang, X. F., Davidovits, P., Smith, K. A., Kolb, C. E., and Worsnop, D. R.: Development of an aerosol mass spectrometer for size and composition analysis of submicron particles, Aerosol Sci. Tech., 33, 49-70, doi: 10.1080/027868200410840, 2000.

Jimenez, J. L., Jayne, J. T., Shi, Q., Kolb, C. E., Worsnop, D. R., Yourshaw, I., Seinfeld, J. H., Flagan, R. C., Zhang, X., Smith, K. A., Morris, J. W., and Davidovits, P.: Ambient aerosol sampling with an Aerosol Mass Spectrometer, J. Geophys. Res.-Atmos., 108, 8425, doi:8410:1029/2001JD001213, 2003.

Jimenez, J. L., Canagaratna, M. R., Donahue, N. M., Prevot, A. S. H., Zhang, Q., Kroll, J. H., DeCarlo, P. F., Allan, J. D., Coe, H., Ng, N. L., Aiken, A. C., Docherty, K. S., Ulbrich, I. M., Grieshop, A. P., Robinson, A. L., Duplissy, J., Smith, J. D., Wilson, K. R., Lanz, V. A., Hueglin, C., Sun, Y. L., Tian, J., Laaksonen, A., Raatikainen, T., Rautiainen, J., Vaattovaara, P., Ehn, M., Kulmala, M., Tomlinson, J. M., Collins, D. R., Cubison, M. J., Dunlea, J., Huffman, J. A., Onasch, T. B., Alfarra, M. R., Williams, P. I., Bower, K., Kondo, Y., Schneider, J., Drewnick, F., Borrmann, S., Weimer, S., Demerjian, K., Salcedo, D., Cottrell, L., Griffin, R., Takami, A., Miyoshi, T., Hatakeyama, S., Shimono, A., Sun, J. Y., Zhang, Y. M., Dzepina, K., Kimmel, J. R., Sueper, D., Jayne, J. T., Herndon, S. C., Trimborn, A. M., Williams, L. R., Wood, E. C., Middlebrook, A. M., Kolb, C. E., Baltensperger, U., and Worsnop, D. R.: Evolution of organic aerosols in the atmosphere, Science, 326, 1525-1529, doi: 10.1126/science.1180353, 2009.

Kaltsonoudis, C., Kostenidou, E., Louvaris, E., Psichoudaki, M., Tsiligiannis, E., Florou, K., Liangou, A., and Pandis, S. N.: Characterization of fresh and aged organic aerosol emissions from meat charbroiling, Atmos. Chem. Phys., 17, 7143-7155, doi: org/10.5194/acp-17-7143-2017, 2017.

Kim, H., Zhang, Q., Bae, G. N., Kim, J. Y., and Lee, S. B.: Sources and atmospheric processing of winter aerosols in Seoul, Korea: insights from real-time measurements using a high-resolution aerosol mass spectrometer, Atmos. Chem. Phys., 17, 2009-2033, doi:10.5194/acp-17-2009-2017, 2017.

Klein, F., Farren, N. J., Bozzetti, C., Daellenbach, K. R., Kilic, D., Kumar, N. K., Pieber, S. M., Slowik, J. G., Tuthill, R. N., Hamilton, J. F., Baltensperger, U., Prévôt, A. S. H., and El Haddad, I.: Indoor terpene emissions from cooking with herbs and pepper and their secondary organic aerosol production potential, Sci. Rep., 6, 36623, doi: 10.1038/srep36623, 2016.

Kleindienst, T. E., Jaoui, M., Lewandowski, M., Offenberg, J. H., Lewis, C. W., Bhave, P. V. and Edney, E. O.: Estimates of the contributions of biogenic and anthropogenic hydrocarbons to secondary organic aerosol at a southeastern US location, Atmos. Environ., 41, 8288-8300, doi: 10.1016/j.atmosenv.2007.06.045, 2007.

Knote, C., Brunner, D., Vogel, H., Allan, J., Asmi, A., Äijälä, M., Carbone, S., van der Gon, H. D., Jimenez, J. L., Kiendler-Scharr, A., Mohr, C., Poulain, L., Prévôt, A. S. H., Swietlicki, E., and Vogel, B.: Towards an online-coupled chemistry-climate model: evaluation of trace gases and aerosols in COSMO-ART, Geosci. Model Dev., 4, 1077–1102, doi: org/10.5194/gmd-4-1077-2011, 2011.

Kroll, J. H., Donahue, N. M., Jimenez, J. L., Kessler, S. H., Canagaratna, M. R., Wilson, K. R., Altieri, K. E., Mazzoleni, L. R., Wozniak, A. S., Bluhm, H., Mysak, E. R., Smith, J. D., Kolb, C. E., and Worsnop, D. R.: Carbon oxidation state as a metric for describing the chemistry of atmospheric organic aerosol, Nat. Chem., 3, 133-139, doi: 10.1038/nchem.948, 2011.

Lanz, V. A., Alfarra, M. R., Baltensperger, U., Buchmann, B., Hueglin, C., and Prévôt, A. S. H.: Source apportionment of submicron organic aerosols at an urban site by factor analytical modelling of aerosol mass spectra, Atmos. Chem. Phys., 7, 1503-1522, doi:10.5194/acp-7-1503-2007, 2007.

Lanz, V. A., Alfarra, M. R., Baltensperger, U., Buchmann, B., Hueglin, C., Szidat, S., Wehrli, M. N., Wacker, L., Weimer, S., Caseiro, A., Puxbaum, H., and Prevot, A. S. H.: Source attribution of submicron organic aerosols during wintertime inversions by advanced factor analysis of aerosol mass spectra, Environ. Sci. Technol., 42, 214–220, doi:10.1021/es0707207, 2008.

Lee, B. P., Li, Y. J., Yu, J. Z., Louie, P. K., and Chan, C. K.: Characteristics of submicron particulate matter at the urban roadside in downtown Hong Kong- Overview of 4 months of continuous high-resolution aerosol mass spectrometer measurements, J. Geophys. Res., 120, 7040-7058, doi: 10.1002/2015JD023311, 2015.

Lee, B. P., Louie, P. K. K., Luk, C., and Chan, C. K.: Evaluation of traffic exhaust contributions to ambient carbonaceous submicron particulate matter in an urban roadside environment in Hong Kong, Atmos. Chem. Phys., 17, 15121-15135, doi: doi.org/10.5194/acp-17-15121-2017, 2017.

Li, Y. J., Lee, B. Y. L., Yu, J. Z., Ng, N. L., and Chan, C. K.: Evaluating the degree of oxygenation of organic aerosol during foggy and hazy days in Hong Kong using high-resolution time-of-flight aerosol mass spectrometry (HR-ToF-AMS), Atmos. Chem. Phys., 13, 8739-8753, doi: 10.5194/acp-13-8739-2013, 2013.

Li, Y. J., Lee, B. P., Su, L., Fung, J. C. H., and Chan, C. K.: Seasonal characteristics of fine particulate matter (PM) based on high-resolution time-of-flight aerosol mass spectrometric (HR-ToF-AMS) measurements at the HKUST Supersite in Hong Kong, Atmos. Chem. Phys., 15, 37-53, doi: 10.5194/acp-15-37-2015, 2015.

Liu, T., Liu, Q., Li, Z., Huo, L., Chan, M., Li, X., Zhou, Z. and Chan, C. K.: Emission of volatile organic compounds and production of secondary organic aerosol from stir-frying spices, Sci. Total Environ., 599-600, 1614-1621, doi: 10.1016/j.scitotenv.2017.05.147, 2017a.

Liu, T., Li, Z., Chan, M., and Chan, C. K.: Formation of secondary organic aerosols from gas-phase emissions of heated cooking oils, Atmos. Chem. Phys., 17, 7333-7344, doi: 10.5194/acp-17-7333-2017, 2017b.

Liu, T., Wang, Z., Huang, D. D., Wang, X. and Chan, C. K.: Significant production of secondary organic aerosol from emissions of heated cooking oils, Environ. Sci. Technol. Lett., 5, 32-37, doi: doi.org/10.1021/acs.estlett.7b00530, 2018.

Liu, T., Zhou, L., Liu, Q., Lee, B. P., Yao, D., Lu, H., Lyu, X., Guo, H., and Chan, C. K.: Secondary organic aerosol formation from urban roadside air in Hong Kong, Environ. Sci. Technol., 53, 3001-3009, doi: 10.1021/acs.est.8b06587, 2019.

Louie, P. K., Watson, J. G., Chow, J. C., Chen, A., Sin, D. W., and Lau, A. K.: Seasonal characteristics and regional transport of $PM_{2.5}$ in Hong Kong, Atmos. Environ., 39, 1695-1710, doi: 10.1016/j.atmosenv.2004.11.017, 2005.

Lyu, X.P., Guo, H., Simpson, I. J., Meinardi, S., Louie, P. K., Ling, Z.H., Wang, Y., Liu, M., Luk, C.W.Y., Wang, N., and Blake, D. R.: Effectiveness of replacing catalytic converters in LPG-fueled vehicles in Hong Kong, Atmos. Chem. Phys., 16, 6609-6626, doi: org/10.5194/acp-16-6609-2016, 2016.

Lyu, X. P., Zeng, L. W., Guo, H., Simpson, I. J., Ling, Z. H., Wang, Y., Murray, F., Louie, P. K. K., Saunders, S. M., Lam, S. H. M. and Blake, D. R.: Evaluation of the effectiveness of air pollution control measures in Hong Kong, Environ. Pollut., 220, 87-94, doi: 10.1016/j.envpol.2016.09.025, 2017a.

Lyu, X. P., Guo, H., Cheng, H. R., Wang, X. M., Ding, X., Lu, H. X., YAO, D. W. and Xu, C.: Observation of SOA tracers at a mountainous site in Hong Kong: Chemical characteristics, origins and implication on particle growth, Sci. Total Environ., 605, 180-189, doi: 10.1016/j.scitotenv.2017.06.161, 2017b.

Middlebrook, A. M., Bahreini, R., Jimenez, J. L., and Canagaratna, M. R.: Evaluation of composition-dependent collection efficiencies for the Aerodyne Aerosol Mass Spectrometer using field data, Aerosol Sci. Tech., 46, 258–271, doi:10.1080/02786826.2011.620041, 2012.

Mohr, C., Huffman, J. A., Cubison, M. J., Aiken, A. C., Docherty, K. S., Kimmel, J. R., Ulbrich, I. M., Hannigan, M., and Jimenez, J. L.: Characterization of primary organic aerosol emissions from meat cooking, trash burning, and motor vehicles with high-resolution aerosol mass spectrometry and comparison with ambient and chamber observations, Environ. Sci. Technol., 43, 2443–2449, doi:10.1021/es8011518, 2009.

Mohr, C., DeCarlo, P. F., Heringa, M. F., Chirico, R., Slowik, J. G., Richter, R., Reche, C., Alastuey, A., Querol, X., Seco, R., Peñuelas, J., Jiménez, J. L., Crippa, M., Zimmermann, R., Baltensperger, U., and Prévôt, A. S. H.: Identification and quantification of organic aerosol from cooking and other sources in Barcelona using aerosol mass spectrometer data, Atmos. Chem. Phys., 12, 1649–1665, doi:10.5194/acp-12-1649-2012, 2012.

Ng, N. L., Canagaratna, M. R., Zhang, Q., Jimenez, J. L., Tian, J., Ulbrich, I. M., Kroll, J. H., Docherty, K. S., Chhabra, P. S., Bahreini, R., Murphy, S. M., Seinfeld, J. H., Hildebrandt, L., Donahue, N. M., DeCarlo, P. F., Lanz, V. A., Prévôt, A. S. H., Dinar, E., Rudich, Y., and Worsnop, D. R.: Organic aerosol components observed in Northern Hemispheric datasets from Aerosol Mass Spectrometry, Atmos. Chem. Phys., 10, 4625-4641, doi: 10.5194/acp-10-4625-2010, 2010.

Ng, N. L., Canagaratna, M. R., Jimenez, J. L., Chhabra, P. S., Seinfeld, J. H., and Worsnop, D. R.: Changes in organic aerosol composition with aging inferred from aerosol mass spectra, Atmos. Chem. Phys., 11, 6465-6474, doi: 10.5194/acp-11-6465-2011, 2011.

Nordin, E. Z., Eriksson, A. C., Roldin, P., Nilsson, P. T., Carlsson, J. E., Kajos, M. K., Hellén, H., Wittbom, C., Rissler, J., Löndahl, J., Swietlicki, E., Svenningsson, B., Bohgard, M., Kulmala, M., Hallquist, M. and Pagels, J. H.: Secondary organic aerosol formation from idling gasoline passenger vehicle emissions investigated in a smog chamber. Atmos. Chem. Phys., 13, 6101-6116, doi: 10.5194/acp-13-6101-2013, 2013.

Offenberg, J. H., Lewis, C. W., Lewandowski, M., Jaoui, M., Kleindienst, T. E. and Edney, E. O.: Contributions of toluene and α-pinene to SOA formed in an irradiated toluene/α-pinene/NOx/air mixture: comparison of results using 14C content and SOA organic tracer methods, Environ. Sci. Technol., 41, 3972-3976, doi: 10.1021/es070089+, 2007.

Paatero, P. and Tapper, U.: Positive matrix factorization- A nonnegative factor model with optimal utilization of error-Estimates of data values, Environmetrics, 5, 111- 126, doi:10.1002/env.3170050203, 1994.

Pagonis, D.; Krechmer, J. E.; de Gouw, J.; Jimenez, J. L. and Ziemann, P. J.: Effects of gas−wall partitioning in Teflon tubing and instrumentation on time-resolved measurements of gas-phase organic compounds, Atmos. Meas. Tech. 10, 4687−4696, doi: 10.5194/amt-10-4687-2017, 2017.

Pope, C.A. and Dockery, D.W.: Health effects of fine particulate air pollution: lines that connect, J. Air Waste Manage. Assoc., 56, 709-742, doi: 10.1080/10473289.2006.10464485, 2006.

Qin, Y. M., Li, Y. J., Wang, H., Lee, B. P., Huang, D. D. and Chan, C. K.: Particulate matter (PM) episodes at a suburban site in Hong Kong: evolution of PM characteristics and role of photochemistry in secondary aerosol formation, Atmos. Chem. Phys., 16, 14131-14145, doi: 10.5194/acp-16-14131-2016, 2016.

Racherla, P. N., and Adams, P. J.: Sensitivity of global tropospheric ozone and fine particulate matter concentrations to climate change, J. Geophys. Res., 111, D24, doi:10.1029/2005JD006939, 2006.

Setyan, A., Zhang, Q., Merkel, M., Knighton, W. B., Sun, Y., Song, C., Shilling, J. E., Onasch, T. B., Herndon, S. C.,Worsnop, D. R., Fast, J. D., Zaveri, R. A., Berg, L. K., Wiedensohler, A., Flowers, B. A., Dubey, M. K., and Subramanian, R.: Characterization of submicron particles influenced by mixed biogenic and anthropogenic emissions using high-resolution aerosol mass spectrometry: results from CARES, Atmos. Chem. Phys., 12, 8131–8156, doi: 10.5194/acp-12-8131-2012, 2012.

So, K. L., Guo, H., and Li, Y. S.: Long-term variation of $PM_{2.5}$ levels and composition at rural, urban and roadside sites in Hong Kong: Increasing impact of regional air pollution, Atmos. Environ., 41, 9427-9434, doi: 10.1016/j.atmosenv.2007.08.053, 2007.

Sun, C., Lee, B. P., Huang, D., Li, Y. J., Schurman, M. I., Louie, P. K., Luk, C., and Chan, C. K.: Continuous measurements at the urban roadside in an Asian megacity by Aerosol Chemical Speciation Monitor (ACSM): particulate matter characteristics during fall and winter seasons in Hong Kong. Atmos. Chem. Phys., 16, 1713-1728, doi: org/10.5194/acp-16-1713-2016, 2016.

Sun, J., Zhang, Q., Canagaratna, M. R., Zhang, Y., Ng, N. L., Sun, Y., Jayne, J. T., Zhang, X., Zhang, X., and Worsnop, D. R.: Highly time- and size-resolved characterization of submicron aerosol particles in Beijing using an Aerodyne Aerosol Mass Spectrometer, Atmos. Environ., 44, 131-140, doi: 10.1002/mas.20115, 2010.

Sun, Y. L., Zhang, Q., Schwab, J. J., Demerjian, K. L., Chen, W. N., Bae, M. S., Hung, H. M., Hogrefe, O., Frank, B., Rattigan, O. V., and Lin, Y. C.: Characterization of the sources and processes of organic and inorganic aerosols in New York city with a high-resolution time-of-flight aerosol mass spectrometer, Atmos. Chem. Phys., 11, 1581–1602, doi:10.5194/acp-11-1581- 2011, 2011.

Schauer, J. J., Kleeman, M. J., Cass, G. R., Simoneit, B. R: Measurement of emissions from air pollution sources. 4. C1- C27 organic compounds from cooking with seed oils, Environ. Sci. Technol, 36, 567−575, doi: org/10.1021/es002053m, 2002.

Tai, A. P., Mickley, L. J., and Jacob, D. J.: Correlations between fine particulate matter ($PM_{2.5}$) and meteorological variables in the United States: Implications for the sensitivity of $PM_{2.5}$ to climate change, Atmos. Environ., 44, 3976-3984, doi: 10.1016/j.atmosenv.2010.06.060, 2010.

Ulbrich, I. M., Canagaratna, M. R., Zhang, Q., Worsnop, D. R., and Jimenez, J. L.: Interpretation of organic components from Positive Matrix Factorization of aerosol mass spectrometric data, Atmos. Chem. Phys., 9, 2891-2918, doi:10.5194/acp-9-2891-2009, 2009.

Vu, H. Q., Li, G., Law, R., and Zhang, Y.: Tourist activity analysis by leveraging mobile social media data, J. Travel Res., 57, 883-898, doi: org/10.1177/0047287517722232, 2018.

Wang, Y., Wang, H., Guo, H., Lyu, X, Cheng, H., Ling, Z., Louie, P.K., Simpson, I.J., Meinardi I.J. and Blake, D.R.: Long-term O_3-precursor relationships in Hong Kong: field observation and model simulation, Atmos. Chem. Phys., 17, 10919-10935, doi: org/10.5194/acp-17-10919-2017, 2017.

Xu, L., Pye, H. O. T., He, J., Chen, Y., Murphy, B. N., Ng, N. L.: Experimental and model estimates of the contributions from biogenic monoterpenes and sesquiterpenes to secondary organic aerosol in the southeastern United States, Atmos. Chem. Phys. 18, 12613-12637, doi: org/10.5194/acp-18-12613-2018, 2018.

Yao, D, Lyu, X, Murray, F., Morawska, L., Yu, W., Wang, J., and Guo, H.: Continuous effectiveness of replacing catalytic converters on liquified petroleum gas-fueled vehicles in Hong Kong, Sci. Total Environ., 648, 830-838, doi: org/10.1016/j.scitotenv.2018.08.191, 2019.

Zhao, Y., Hu, M., Slanina, S., and Zhang, Y.: The molecular distribution of fine particulate organic matter emitted from western-style fast food cooking, Atmos. Environ., 41, 8163-8171, doi: org/10.1016/j.atmosenv.2007.06.029, 2007.

Zhang, Q., Alfarra, M. R., Worsnop, D. R., Allan, J. D., Coe, H., Canagaratna, M. R., and Jimenez, J. L.: Deconvolution and quantification of hydrocarbon-like and oxygenated organic aerosols based on aerosol mass spectrometry, Environ. Sci. Technol., 39, 4938–4952, doi:10.1021/es048568l, 2005.

Zhang, Q., Jimenez, J. L., Canagaratna, M. R., Ulbrich, I. M., Ng, N. L., Worsnop, D. R., and Sun, Y.: Understanding atmospheric organic aerosols via factor analysis of aerosol mass spectrometry: a review, Anal. Bioanal. Chem., 401, 3045–3067, doi: 10.1007/s00216-011-5355-y, 2011.

Zhang, X., Xu, J., Kang, S., Zhang, Q., and Sun, J.: Chemical characterization and sources of submicron aerosols in the northeastern Qinghai–Tibet Plateau: insights from high-resolution mass spectrometry, Atmos. Chem. Phys., 19, 7897-7911, doi: 10.5194/acp-19-7897-2019, 2019.